RSC Advances

PAPER

Cite this: *RSC Adv.*, 2016, **6**, 19964

Precise determination of the nanoparticle concentration and ligand density of engineered water-soluble HgSe fluorescent nanoparticles†

Diego Bouzas-Ramos, Mario Menéndez-Miranda, José M. Costa-Fernández,* Jorge Ruiz Encinar* and Alfredo Sanz-Medel

HgSe nanoparticles (NPs) have been recognized as the ultimate product of mercury detoxification in biological systems. However, the exact mechanism of their formation and distribution in animals is not understood, and thus well-characterized engineered NPs would be invaluable to investigate such metabolic products. In this work, HgSe NPs were sonochemically synthesized and transferred for the first time to aqueous media using dihydrolipoic acid (DHLA) as a capping ligand. A thorough characterization of the engineered HgSe NPs was carried out. Different complementary analytical techniques, including high resolution-transmission electron microscopy (HR-TEM) and X-ray powder diffraction (XRD), provided information about the morphology and crystal structure of the NPs. X-ray photoelectron spectroscopy (XPS) and energy dispersive X-ray spectrometer (EDX) analysis were used in order to assess the chemical composition and purity of the same HgSe NPs. Moreover, Fourier transform infrared spectroscopy (FT-IR), nuclear magnetic resonance (NMR), dynamic light scattering (DLS), zeta potential determinations and asymmetric flow field-flow fractionation (AF4) coupled on-line to fluorescence and inductively coupled plasma-mass spectrometry (ICP-MS) detectors confirmed that the DHLA ligands were bound onto the surface of the NPs making them stable in aqueous solutions. Fluorescence measurements evidenced that the engineered NPs exhibit a photoluminescence emission centred at 575 nm. Finally, the Se/Hg molar ratio of the NPs was accurately and precisely determined by ICP-MS to be 0.96 ± 0.03. Such valuable information was used to precisely determine the nanoparticle concentration in aqueous solution (in terms of number of nanoparticles per unit volume) and the ligand density, in terms of number of DHLA molecules per nanoparticle (2500 ± 125).

Received 9th December 2015
Accepted 12th February 2016

DOI: 10.1039/c5ra26268b

www.rsc.org/advances

Introduction

Since the discovery of the protective effect of selenium (Se) on intoxication by mercury (Hg) in laboratory rats,[1] extensive studies have demonstrated the toxicological antagonism between both elements in animals.[2,3] Nowadays it is well-known that the accumulation of Hg often accompanies Se accumulation, typically at a 1 : 1 molar ratio, in tissues of marine mammals[4] and in organs of Hg mine workers.[5] This equimolar Hg : Se ratio might be attributed to the presence of mercury selenide (HgSe) nanoparticles (NPs) in the organs. Actually, HgSe granules were found in the liver of cetaceans and were assumed as the final metabolic product.[6] Further studies proposed that Se-containing biomolecules provide effective and efficient pathways for converting some toxic Hg compounds to chemically and biologically inert HgSe NPs.[7,8] Although the mechanism is still far to be fully understood, these NPs are thought to be the ultimate metabolic product of the Hg detoxification mechanism in biological systems.[7,9] In fact, several studies reported the presence of HgSe NPs in tissues of various marine mammals,[10,11] sea birds[12] and most recently in human brain.[13]

In order to shed new light towards a better understanding of the formation, distribution, metabolism and final fate of HgSe NPs in biological systems, the use of well-characterized water-soluble engineered NPs is needed to initiate basic *in vitro* and *in vivo* studies. In this context, a detailed and comprehensive physicochemical characterization of the engineered NPs is required to ensure comparative and reliable data.[14] When synthesizing novel NPs their full characterization in dry state is still indispensable (*e.g.* size, shape and chemical composition of the core), but their properties in solution (*e.g.* surface potential and hydrodynamic diameter) must also be carefully characterized in order to understand their behaviour in biological systems.[15,16] Furthermore, it is imperative to determine the nanoparticle concentration in terms of number of NPs in

Department of Physical and Analytical Chemistry, University of Oviedo, Julián Clavería 8, 33006, Oviedo, Spain. E-mail: jcostafe@uniovi.es; ruizjorge@uniovi.es; Tel: +34 985102970

† Electronic supplementary information (ESI) available. See DOI: 10.1039/c5ra26268b

a given sample, since NP toxicity issues are commonly linked to NP concentration-dependent effects.[15]

During the past decades, only a small number of publications are dealing with the synthesis of HgSe NPs. Conventional methods reported for the preparation of mercury chalcogenides include solid state reactions at elevated temperature[17] and reactions of metal cations with hydrogen chalcogenides in aqueous solution.[18] However, the solid-state reactions are not easily controllable, while the use of the gaseous and highly toxic hydrogen chalcogenides has some important practical limitations. Additionally, the obtained products are not nanosized. More recently, preparation of metal chalcogenides has been described by means of a solvothermal synthesis[19] and nanocrystalline mercury chalcogenides using a room-temperature conversion route,[20] for both methods long reaction times are required. Alternatively, the sonochemical method has been recently shown to be a quick and versatile technique to prepare HgSe nanostructures.[21] Because of the unique reaction effect of the ultrasound irradiation, this method has a rapid reaction rate, tuneable reaction conditions and the capacity to form HgSe NPs with uniform shapes, narrow size distributions and high purity.[22,23] The effects of ultrasound result from the process called acoustic cavitation: the formation, growth and implosive collapse of bubbles in a liquid. During the ultrasonic radiation, intense heating of the bubbles occurs.[24] These unique reaction conditions, temperatures of roughly 5000 K and pressures of about 500 bar, provide an ideal atmosphere for the preparation of nanomaterials. While the sonochemical synthesis of HgSe NPs in aqueous solutions has been recently described,[25,26] the final product of the synthesis is essentially insoluble and, furthermore, an appropriate characterization of the obtained NPs is still lacking today.

Herein, we present a simple and comprehensive protocol to produce and thoroughly characterize HgSe NPs in water media ready to be used in environmental and biological studies. A sonochemical synthesis has been employed and the resulting HgSe NPs were then transferred for the first time to aqueous media by capping them with dihydrolipoic acid (DHLA) ligands. Combination of the quantitative data produced by inductively coupled plasma-mass spectrometry (ICP-MS), directly or coupled to a powerful separation technique for NPs (asymmetric flow field-flow fractionation, AF4), with complementary techniques such as Fourier transform infrared spectroscopy (FT-IR), nuclear magnetic resonance (NMR), X-ray powder diffraction (XRD), high resolution-transmission electron microscopy (HR-TEM) and dynamic light scattering (DLS) provided an in-depth characterization of the engineered HgSe NPs produced. In this context, elemental stoichiometry of the core, ligand density on the surface and nanoparticle concentration, in terms of the number of nanoparticles per unit volume, could be precisely determined.

Experimental

Reagents and materials

All the chemical reagents used in the experiments were of analytical grade and used as received without further purification. Deionized ultrapure water (18.2 MΩ cm) was obtained with a Milli-Q system (Millipore, Bedford, MA, USA) and used throughout the work.

The precursors used for the synthesis of the NPs were selenium powder (99.99%) from Sigma-Aldrich (Milwaukee, WI, USA), mercury(II) acetate (≥98%) from Panreac (Barcelona, Spain) and ethylenediaminetetraacetic acid disodium salt dihydrate (EDTA, ≥99%) from Fluka (Basel, Switzerland). Sodium hydroxide and absolute ethanol were obtained from Merck (Darmstadt, Germany) and Sigma-Aldrich, respectively.

Water-solubilization of HgSe NPs was achieved by coating them with DHLA ligands synthesized in our laboratory.[28] For such purpose, DL-thioctic acid (98%), sodium bicarbonate and sodium borohydride (≥96%) were purchased from Acros Organics (Geel, Belgium), Merck and Fluka, respectively. Potassium *tert*-butoxide (≥98%), anhydrous methanol and anhydrous toluene, all of them acquired from Sigma-Aldrich, were also used during the solubilization process. L-Cysteine hydrochloride monohydrate (≥99%) was purchased from Merck. Nitric acid (65%, v/v) from Merck was additionally purified by sub-boiling distillation to operate with the minimum background levels of metallic impurities. External FIA (Flow Injection Analysis) calibrations using Merck certified 1000 mg L^{-1} standards of Se, Hg and S were used in the ICP-MS analysis.

Ammonium acetate and sodium dodecyl sulphate (SDS), from Sigma-Aldrich, were used for the carrier in the AF4 instrument.

Instrumentation

The synthesis of the HgSe NPs was carried out using a Vibra-Cell VC250 high-intensity ultrasonic probe (Sonics & Materials, USA). An ultrasonic bath (JP Selecta, Spain) was used to improve the acid digestion of the DHLA-capped NPs before ICP-MS analysis.

HR-TEM images were obtained on a JEM-2100F (JEOL, Japan) transmission electron microscope with a copper grid, using an accelerating voltage of 200 kV. The JEM-2100F was equipped with an energy dispersive X-ray spectrometer (EDX). XRD measurements were performed using a X'Pert Pro diffractometer (PANalytical, Netherlands). X-ray photoelectron spectroscopy (XPS) analysis was performed using a Phoibos 100 hemispherical analyzer with a MCD-5 detector (SPECS, Germany).

Infrared spectra were taken in a Varian 670 FT-IR spectrometer (Agilent, Australia) equipped with a Golden Gate attenuated total reflectance (ATR) device consisted of a diamond crystal with one internal reflection. Room temperature ^{1}H-NMR spectra were recorded on a Bruker AV-600 spectrometer (600.15 MHz).

Elemental measurements were carried out on a 8800 Triple Quadrupole ICP-MS (Agilent, Japan) using a MicroMist nebulizer. A two-position and six-port Rheodyne injection valve (IDEX Health & Science, Germany) was used to allow an on-line flow injection analysis (FIA) of the samples.

Zeta potential and DLS measurements were carried out with a Zetasizer Nano ZS (Malvern Instruments, UK). All these

measurements were performed using DTS1070 disposable capillary cells and ZEN0040 disposable cuvettes, respectively. UV/vis spectrophotometric measurements were performed in a Genesys 10S Spectrophotometer (Thermo Scientific, Germany). Fluorescence spectra were recorded on a LS-45 Luminescence Spectrophotometer (Perkin Elmer, USA) using a fixed excitation wavelength of 400 nm with both excitation and emission slit width of 10 nm. The measurements of absorbance and fluorescence were carried out using conventional Quartz SUPRASIL cuvettes (Hellma Analytics, Germany). The AF4 system used was an AF2000 (Postnova Analytics, Germany). The fluorescence detector on-line coupled to the AF4 was a 1200 Series FLD (Agilent, Japan).

Experimental procedures

Sonochemical synthesis of HgSe NPs. HgSe NPs were synthesized using Se powder and $Hg(OAc)_2$ as precursors *via* the sonochemical procedure described by Kristl *et al.*[25] with slight modifications. Briefly, 5 mmol of Se powder was dissolved in 50 mL of 5 M NaOH solution. The mixture was irradiated with ultrasounds *via* a direct-immersion high-intensity probe (80 W cm^{-2}) for 30 min, and simultaneously an equimolar amount of Hg^{2+} in a 0.1 M EDTA solution was slowly added. After the EDTA addition, the solution was left irradiated during 3 h at room temperature. After ultrasounds irradiation, the resulting suspension was centrifuged and the black precipitate was washed in sequence with volumes of 0.1 M EDTA, water and absolute ethanol. Finally, the washed powder was left to dry in an open vessel to air.

Preparation of DHLA and transfer of HgSe NPs to aqueous media. Pure DHLA was prepared following the procedure described by Clapp *et al.*[28] Colloidal suspension of water-soluble NPs was prepared by dispersing 20–50 mg of insoluble sonochemically synthesized HgSe in 0.4–1.0 mL of freshly prepared DHLA. The mixture was heated to 80 °C for 2 h while stirring and incubated overnight with agitation. The resulting solution was diluted in 4–5 mL anhydrous methanol and an excess of potassium *tert*-butoxide was slowly added in order to allow the deprotonation of the terminal carboxyl groups on the DHLA. The formed precipitate of DHLA-capped HgSe was sedimented by centrifugation and these new surface-modified NPs with DHLA were dispersed in water (pH $\sim$ 12). An additional purification step, consisting in an ultrafiltration using a 100 kDa cutoff ultracentrifugal filter and the subsequent resuspension of capped NPs in alkaline water (pH > 7) was required to remove excess of reagents. Experimental conditions used for ultrafiltration were 5000 rpm and 5 min ($\times$5 cycles).

XRD and XPS measurements. For indexing and microstructural analysis of the synthesized HgSe NPs, X-ray powder diffraction measurements were performed employing a X'Pert Pro diffractometer with Bragg–Brentano configuration. This powder diffractometer was equipped with a Johansson Ge(111) monochromator producing a monochromatic Cu $K_{\alpha 1}$ radiation ($\lambda = 1.5405982$ Å) and a PIXcel detector. The powder sample was placed on a zero-background silicon sample holder. XRD pattern from 20° to 100° (2θ) were recorded at room temperature with a step size of 0.053° (2θ) and a counting time of 500 s per step.

XPS measurements of the HgSe NPs powder were performed under ultra-high vacuum conditions (10^{-9} to 10^{-10} mbar) using Mg X-ray radiation (1253.6 eV) at 200 W. Low resolution spectrum was taken with pass energy of 90 eV, whereas high resolution spectra were recorded at pass energy of 30 eV. Analysis of the spectra was performed using the Computer Aided Surface Analysis for X-ray Photoelectron Spectroscopy software (CasaXPS).

ICP-MS analysis. Simultaneous detection of Se, Hg and S was carried out with a ICP-MS equipped with a triple quadrupole,[29] due to its capabilities to detect, free of interference and with high sensitivity, typically highly interfered elements such as Se and especially S.[30] For such purpose, oxygen was introduced in the collision/reaction cell at a flow rate of 0.35 mL min^{-1}. Se and S were detected in mass shift MS/MS mode ($^{80}Se^+ \rightarrow {}^{96}SeO^+$ and $^{32}S^+ \rightarrow {}^{48}SO^+$, respectively) after their reaction with oxygen in the cell. Hg, which does not react with oxygen, was measured in on-mass MS/MS mode ($^{202}Hg^+ \rightarrow {}^{202}Hg^+$). The integration time for the targeted isotopes ^{76}Se, ^{78}Se, ^{80}Se, ^{200}Hg, ^{202}Hg, ^{32}S and ^{34}S was 0.1 s. Each operation conditions were daily optimized using a tuning solution. Integration of the FIA peaks was performed using the MassHunter software (Agilent). ICP-MS operating conditions are summarized in Table S1 (see ESI†).

Elemental ratios (Se/Hg and Se/S) in the DHLA–HgSe NPs were determined by performing first an external FIA calibration using Se, Hg and S standards (see Fig. S1 and S2 in the ESI†). A 0.1% (w/v) solution of cysteine in 1% nitric acid was used as carrier for the determination of the Se/Hg ratio. The addition of cysteine to the carrier during the measurement of the Se/Hg ratio was essential to eliminate any adsorption of mercury or memory effects in the ICP-MS.[31] Conversely, a 1% nitric acid solution was used as carrier for the determination of the Se/S ratio inasmuch as sulphur detection would have not been possible if cysteine was present in the carrier. For the determination of these elemental molar ratios, the synthesized DHLA–HgSe NPs were injected directly to the ICP-MS. The experimentally obtained Se/Hg and Se/S area ratios could be then translated into the Se/Hg and Se/S molar ratios using the corresponding elemental calibration curves previously obtained.

In order to measure the total mass of Hg, Se and S in the given sample, a complete digestion of the DHLA-capped HgSe NPs was needed and the ICP-MS measurements were performed as described above. The total mass of Hg and S and the determined elemental molar ratios were used for the determination of the nanoparticle concentration and the ligand density of the NPs. Aqua regia was used to perform the digestion of the NPs solution. A purification step before digestion was required to remove the possible excess of DHLA in solution by ultrafiltration using a 100 kDa cutoff membrane filter, at 5000 rpm and 5 min ($\times$3 cycles).

AF4-fluorescence-ICP-MS analysis. A 2 g L^{-1} ammonium acetate, with 0.01% (w/v) of SDS, buffered solution (pH 10) was employed as carrier in the AF4 system.

After fractionation, the effluent was first directed to the fluorescence detector (being operated at an excitation wavelength of 400 nm and at emission wavelength of 575 nm) and then on-line to the ICP-MS detector equipped with a triple quadrupole. Experimental conditions for the AF4 separation of the DHLA–HgSe NPs are summarized in Table S2 (see ESI†). ICP-MS operating conditions are the same as in the ICP-MS analysis section, but in this experiment only Se and Hg were monitored because S detection was hampered by the use of the required SDS. Se/Hg molar ratio of the on-line separated engineered NPs was determined by external FIA calibration using inorganic standards of Hg and Se.

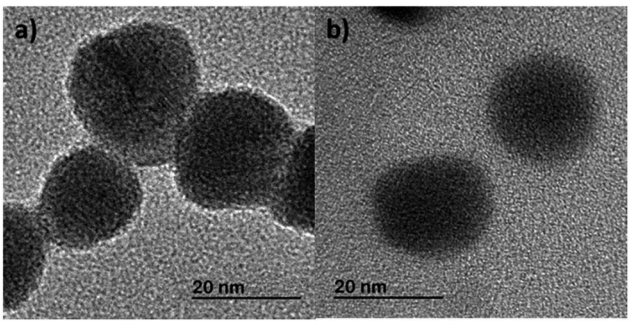

Fig. 1 HR-TEM images of the (a) HgSe NPs, and (b) DHLA-capped HgSe NPs.

Results and discussion

Sonochemical synthesis of HgSe NPs

The synthesis of the HgSe NPs was attempted here employing a sonochemical approach[25] and using Se and $Hg(OAc)_2$ as metal precursors as described in the Experimental section. The mechanism of the sonochemical formation of HgSe NPs is probably related to the radical species generated from water molecules ultrasound energy absorption, eqn (1) below. The extreme conditions occurring during the ultrasound irradiation in aqueous solutions lead to the formation of $H^{\bullet}$ and $OH^{\bullet}$ radicals.[32] While the exact mechanism is still a subject of speculation, a likely reaction mechanism can be as follows:

$$H_2O \rightarrow H^{\bullet} + OH^{\bullet} \quad (1)$$

$$Se^0 + 2OH^- + 2H^{\bullet} \rightarrow Se^{2-} + 2H_2O \quad (2)$$

$$Hg(OAc)_2 + EDTA \rightarrow [Hg(EDTA)]^{2+} + 2OAc^- \quad (3)$$

$$[Hg(EDTA)]^{2+} + Se^{2-} \rightarrow HgSe + EDTA \quad (4)$$

That is, the $H^{\bullet}$ radicals generated from the water would be able to reduce Se^0 into Se^{2-} (eqn (2)) that quickly combine with $[Hg(EDTA)]^{2+}$ ions present in solution giving rise to HgSe NPs, as shown in eqn (4). The complexing agents, *e.g.* EDTA, plays a crucial role in the formation of HgSe NPs, since they form a stable complex with Hg^{2+} that could affect the nucleation rate and growth of the NPs.[23] In this sense, it is the EDTA complex that releases Hg^{2+} for the reaction with Se^{2-} and bringing about HgSe nanoparticles, while preventing the formation of HgO.[25]

The actual formation of the HgSe NPs was confirmed by HR-TEM. A nanoparticle population in the purified product, after the synthesis reaction, with a size of 23 ± 2 nm (1SD, $n = 50$) was observed (Fig. S3 in the ESI†). An HR-TEM image of the corresponding HgSe NPs can be seen in Fig. 1a, which shows the presence of NPs with spherical shape and low polydispersity.

HgSe NPs crystal structure and purity estimation

The phase purity and crystal structure of the resulting products were characterized by powder XRD analysis. The XRD pattern of the HgSe is shown in Fig. 2. The intense and sharp diffraction peaks indicates that the obtained nanosized particles were well crystallized. All of the reflections of the pattern can be indexed to the standard peaks of the pure cubic phase of HgSe (tiemannite) with lattice constants of $a = b = c = 0.6085$ nm (space group $F\bar{4}3m$), in good agreement with the reported pattern JCPDS no. 03-065-9275. No peaks of any other phases were detected, indicating the high purity of the product. The nanocrystal size, τ, was also calculated from the three major diffraction peaks of the XRD pattern using the Scherrer equation given in (5):

$$\tau = (K\lambda)/(\beta \cos \theta) \quad (5)$$

where K is the so-called shape factor, which usually takes a value of *ca.* 0.9; λ is the X-ray wavelength used (1.5405982 Å); β is the width of the observed diffraction line at its half intensity maximum (FWHM), in rad; θ is the Bragg angle, in rad.[21] The calculated nanoparticle size was 23 ± 1 nm (1SD, $n = 3$), a value in good agreement with those observed previously by HR-TEM. We could also estimate that the total number of atoms in a HgSe nanoparticle of 23 nm is about 226 000 atoms using the volume of the unit cell.

XPS measurements may provide further information about the composition and purity of the obtained HgSe NPs. The low resolution XPS spectrum of the sample is shown in Fig. 3a. No peaks from eventual impurities present in the sample were observed. The high resolution XPS spectra taken for Hg4f and Se3d regions are shown in Fig. 3b and c, respectively. The two strong peaks detected at 100.6 and 104.6 eV were assigned to the

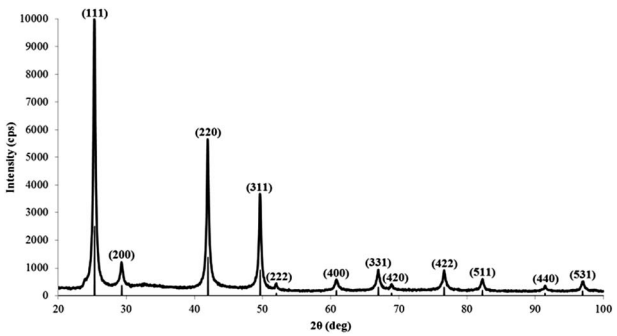

Fig. 2 Powder XRD pattern of the engineered HgSe NPs. The vertical lines indicate the diffraction peak characteristics of the pure cubic tiemannite structure (JCPDS no. 03-065-9275).

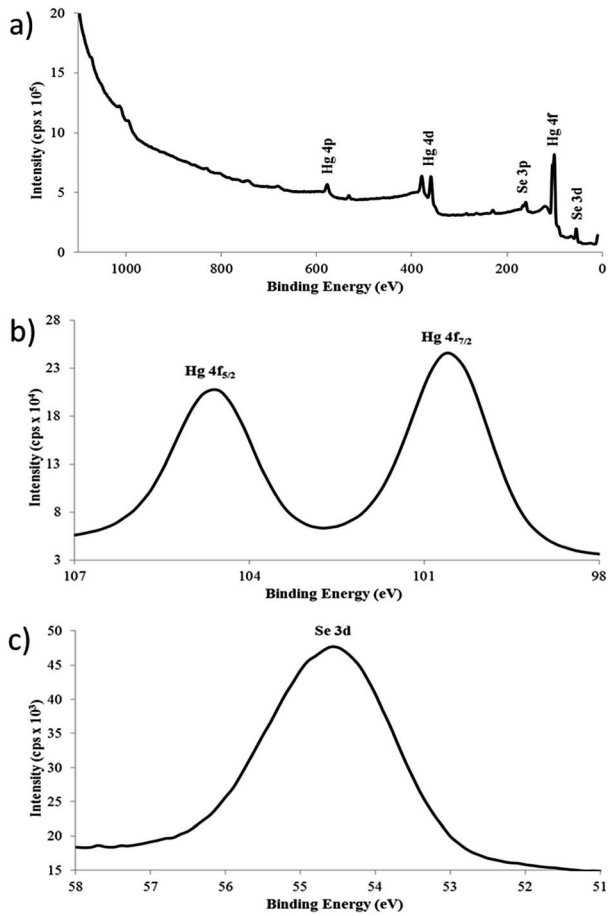

Fig. 3 (a) Low resolution XPS spectrum of the HgSe NPs. High resolution XPS spectra of the (b) Hg4f, and (c) Se3d.

Hg4f binding energy and the peak at 54.6 eV corresponded to the Se3d transition.

Peak areas of Hg4f and Se3d were measured and the quantification of the peaks showed that the Hg : Se atomic ratio was approximately 56 : 44. This result seems to point out that the engineered NPs have a slight excess of Hg, a feature that have already been observed for these type of NPs.[23,25] Unfortunately, accuracy associated was very high (10% as provided by the instrument supplier).

Solubilization and characterization of DHLA-capped HgSe NPs

As previously described, the capping of the HgSe NPs, to turn them stable in aqueous media and compatible with bioanalytical applications, was carried out with DHLA as surface ligands anchored onto the surface of the HgSe NPs through the two sulphur atoms of their thiol (mercapto) groups.[33] Binding of DHLA to the HgSe NPs was driven by favourable interactions between thiol groups of the bidentate ligands and the inorganic surface of the NPs. This modification provides the NP surface with hydrophilic end groups, rendering them stable in aqueous environments. Such mechanism is similar to what has been already reported for CdSe/ZnS quantum dots.[28] The HR-TEM image of the DHLA-capped HgSe is shown in Fig. 1b, which shows that the synthesized DHLA-capped NPs were spherical and well dispersed. Also, compared to the original NPs, no significant change or modification in the HgSe nanoparticle cores was observed.

Both the native HgSe and the DHLA-capped NPs were then characterized by DLS in order to investigate their corresponding size distribution and hydrodynamic diameter. The hydrodynamic diameter increased from 71 ± 1 nm (1SD, $n = 5$) for native HgSe to 78 ± 2 nm (1SD, $n = 5$) for DHLA-capped NPs (see Fig. S4 in the ESI†). This increase can be assigned to the contribution of the DHLA capping to the surface coating. It should be considered that DLS provides information about the hydrodynamic diameter of dispersed NPs. Therefore, it takes into account not only the NP core but also the ligand and the solvatation layers. This explains the significant differences observed with data provided by HR-TEM and XRD (only diameter of the inorganic HgSe core is given here). The polydispersity index (PdI), which indicates the variability in the particle size in a given sample, was also assessed using DLS. Results showed that the performed sonochemical synthesis of HgSe NPs provided a single distribution with an adequate PdI of 0.15 ± 0.02 (1SD, $n = 5$). The PdI of the DHLA-capped NPs was 0.10 ± 0.02 (1SD, $n = 5$), indicating a significant lower polydispersity of the colloidal suspension of capped NPs. Such decrease of the PdI value likely points to an electrostatic stabilization of the DHLA-capped HgSe NPs in aqueous solution *via* the negatively charged carboxylate groups of the DHLA ligands attached on the surface. This results in significant nanoparticle repulsion and therefore less aggregation.

In this context, the zeta potential is an important tool for understanding the state of the nanoparticle surface and so predicting the colloidal stability of NPs (which should be small enough to remain as a stable colloidal suspension). Zeta potential measurements of the DHLA-capped HgSe NPs were carried out at different pH values ranging from 7 to 12, as DHLA-capped NPs are stable in alkaline aqueous media (pH > 7).[28] All the zeta potential values of the DHLA–HgSe NPs in the selected pH range were lower than −35 mV, being more negative values when increasing the pH (see Fig. S5 in the ESI†). Therefore, DHLA-capped HgSe NPs exhibited high colloidal stability in the assayed aqueous solutions.[34] The obtained negative zeta potential values also agreed well with the negative surface charge provided by carboxylate-terminated DHLA ligands. It is worth noting here that DHLA-capped HgSe NPs were stable at such basic pH aqueous medium for *ca.* several weeks, before any visual precipitation was observed.

Additionally, FT-IR spectroscopy and NMR were used to confirm that the DHLA ligands were attached to the surface of the DHLA-capped HgSe NPs. FT-IR spectra of both native and capped HgSe NPs were collected in the spectral range between 600 and 4000 cm^{-1} (see Fig. S6 in the ESI†). Several spectral bands characteristic of the DHLA, such as the symmetric and antisymmetric stretching vibration of $-CH_2-$ at 2920 and 2845 cm^{-1}, the deformation vibration of $-CH_2-$ group at 1415 cm^{-1} and the stretching vibration of C–S at 660 cm^{-1}, are only present in the FT-IR spectrum of the DHLA-capped HgSe

NPs. All of these bands are attributed to the DHLA capping groups.[35]

Furthermore, ^{1}H-NMR spectra of the free DHLA and DHLA–HgSe NPs (Fig. S7 in the ESI†) verified the binding of the thiol groups of DHLA to the surface of the NPs. As can be seen (Fig. S7b†), the two thiol resonance peaks at 1.2–1.3 ppm in the spectrum of free DHLA, which are characteristic of the reduced dithiol moiety,[36] are not present in the DHLA–HgSe NPs spectrum (Fig. S7a†). The other peaks between 1.3 and 2.7 ppm (characteristic of the rest of the DHLA ligand) remained intact after the surface modification of the NPs, except for a small shift which is attributed to a change in its environment.[36]

Finally, EDX analysis was employed to determine the composition of both native and capped HgSe NPs. The EDX spectrum obtained for the native HgSe NPs (Fig. S8a in the ESI†) only exhibited peaks corresponding to Se (47 ± 1%; 1SD, $n = 3$) and Hg (53 ± 1%; 1SD, $n = 3$) in an equimolar mixture. In contrast, the EDX pattern of the DHLA-capped HgSe (Fig. S8b in the ESI†) showed that these NPs were composed not only of Se (47.0 ± 1.0%; 1SD, $n = 3$) and Hg (50.5 ± 2.1%; 1SD, $n = 3$) but also of S (2.5 ± 1.2%; 1SD, $n = 3$). These results confirmed that, as expected, the DHLA molecules were successfully incorporated to the surface of the HgSe NPs and the products are rather pure as shown by the absence of impurity peaks in Fig. S8† (Cu signal comes from the grid used as sample holder).

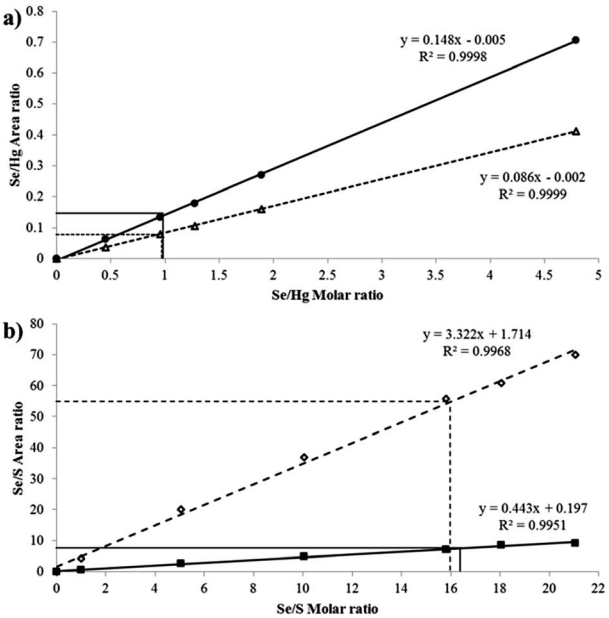

Fig. 4 (a) Plot of the Se/Hg area ratio experimentally obtained by ICP-MS *versus* the theoretical Se/Hg molar ratio for the six elemental standards mixtures prepared. Two independent area elemental ratios were measured in the DHLA–HgSe NPs: (●) ^{80}Se/^{202}Hg and (△) ^{78}Se/^{200}Hg. (b) Plot of the Se/S area ratio experimentally obtained by ICP-MS *versus* the theoretical Se/S molar ratio for the seven elemental standards mixtures prepared. Two independent area elemental ratios were measured in the DHLA-capped HgSe NPs: (◇) ^{76}Se/^{34}S and (■) ^{78}Se/^{32}S. RSD values were below 3% in each point of the calibration curves.

Elemental analysis of DHLA–HgSe NPs

The determination of elemental stoichiometry of the NPs, ligand density and nanoparticle concentration relies on the simultaneous quantification of Hg, Se and S of the DHLA-capped HgSe NPs by triple quadrupole ICP-MS. It is worth mentioning that the standard deviation (SD) associated to each result provided all along the following sections corresponds to the propagated uncertainty of different replicates, considering uncertainties associated to each value used in the corresponding computation.

The inherent quantitative character of the ICP-MS response for precise multielemental characterization of nanostructures[37] enabled us to determine accurately and more precisely the elemental stoichiometry of the DHLA-capped HgSe NPs. The Se/Hg molar ratio was directly determined in a colloidal suspension of DHLA–HgSe NPs, in order to avoid any potential losses or contaminations during acidic digestion. The measured ^{80}Se/^{202}Hg area ratio was then translated into a Se/Hg molar ratio (0.96 ± 0.02 for ^{80}Se/^{202}Hg; 1SD, $n = 4$) using a calibration curve obtained with Se and Hg standard solutions (Fig. 4a). It must be noted that possible differences between the nebulization efficiency of the NPs and the ICP standards should not affect the accuracy of the measured values because ratios were used instead of absolute intensities.[29] Multi-isotope capabilities of ICP-MS allowed measuring an alternative isotope ratio ^{78}Se/^{200}Hg in order to internally validate the result and check for possible interferences. The Se/Hg molar ratio obtained from ^{78}Se/^{200}Hg measurement (0.96 ± 0.01; 1SD, $n = 4$) was identical to the value obtained by measuring the most abundant ^{80}Se/^{202}Hg and closely matched with the predicted value for a tiemannite crystal structure (space group $F\bar{4}3m$) with a 1 : 1 (Se : Hg) stoichiometry.

Interestingly, the use of the ICP-MS equipped with a triple quadrupole analyser allowed the measurement of the low abundant S present after DHLA derivatization, typically highly interfered by ICP-MS.[29,30] In a similar way, a Se/S molar ratio of 16.2 ± 0.6 was obtained for the DHLA–HgSe NPs using a calibration curve built from the adequate S and Se ICP standards (see Fig. 4b). Similarly to the Se/Hg molar ratio determination, two independent Se/S isotope ratios were measured: 16.5 ± 0.3 for ^{78}Se/^{32}S (1SD, $n = 4$) and 16.0 ± 0.5 for ^{76}Se/^{34}S (1SD, $n = 4$). Besides, the elemental composition of the engineered NPs was calculated using the Se/Hg (0.96 ± 0.03) and Se/S (16.2 ± 0.6) molar ratios determined above. The obtained composition for the DHLA–HgSe NPs was 49.5 ± 2.4% of Hg, 47.5 ± 2.3% of Se and 2.93 ± 0.14% of S, values in accordance to the previous observed EDX results. It is worth highlighting that expanded uncertainties for both elemental ratios and composition were below 4 and 5% RSD, respectively.

Determination of the nanoparticle concentration

As said before, the described nanoparticle synthesis produced spherical NPs with a diameter of 23 ± 1 nm. Thus, the volume of each individual spherical nanoparticle was theoretically calculated. Alternatively, the total volume of HgSe NPs was calculated as well from the total mass of Hg measured by ICP-

MS and, using the molar ratio Se/Hg previously determined, the mass of Se.

Once the total mass of NPs has been computed and using the HgSe density (*i.e.* 8.23 g cm^{-3}) it is possible to calculate the total volume of the HgSe NPs in given sample. Nanoparticle concentration in the measured sample could then be estimated dividing such total NP volume by the individual NP volume.

Nanoparticle concentration is a critical and very important parameter to be measured for downstream applications.[15] It is evident that concentrations calculated exclusively in terms of mass of solid in a given volume of solution provides a very limited information. Toxicological effects it would depend on the number of NPs and their size polydispersity more than NP mass. Using ICP-MS results and assuming that the water-solubilized HgSe NPs in the measured sample were spherical with an average diameter of 23 nm (HR-TEM and XRD results), a nanoparticle concentration of 9.5 ± 0.5 nM (1SD, $n = 8$), that corresponds to 57 × 10^{11} NPs per mL, was determined in the solution of DHLA-capped HgSe NPs measured.

Of course, the number of atoms per HgSe nanoparticle could be easily determined as well. In this way the number of atoms per HgSe nanoparticle could be precisely computed, 222 000 ± 8400 atoms (1SD, $n = 8$). This value was in accordance with the theoretical number of atoms per nanoparticle estimated previously by XRD.

Determination of the ligand density

The same digested solution of the capped NPs has been used for the quantification of the nanoparticle ligand density which is of great importance, as well as technically challenging,[27] since it will determine NP stability and reactivity in different media. In this context, the number of DHLA molecules per HgSe nanoparticle was also computed using the total number of NPs, calculated as described above, and the total mass of S measured by the ICP-MS. A purification step before the digestion of the NPs and the subsequent ICP-MS measurement was performed by ultrafiltration to remove the possible excess of DHLA in solution. Once the total number of S atoms per NP was determined and taking into account that each DHLA molecule has two atoms of S, the ligand density calculated for the DHLA-capped HgSe NPs sample was 2500 ± 125 molecules of DHLA per nanoparticle (1SD, $n = 8$).

Again, the expanded uncertainty (5% RSD) was estimated taking into account the corresponding uncertainties associated to the moles of NPs and S present in the solution.

Optical characterization of the DHLA-capped HgSe NPs solution

The optical properties of the engineered NPs in aqueous solution were first evaluated by their UV-vis absorbance and fluorescence spectra. Absorption spectrum of the solubilized HgSe NPs was recorded in a water solution of pH 12 and it showed an excitonic shoulder at *ca.* 390 nm (see Fig. 5). Moreover, the synthesized NPs displayed an intense sharp fluorescence emission at 575 nm. Fig. 5 shows the observed fluorescence spectrum of the DHLA-capped HgSe NPs for an excitation wavelength of 400 nm.

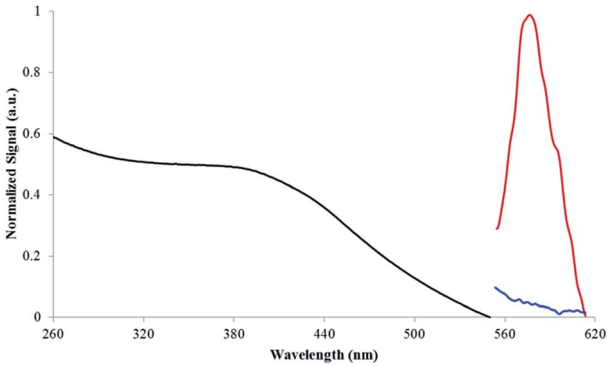

Fig. 5 Fluorescence emission spectra in water media (λ_{ex} = 400 nm) of DHLA-capped HgSe NPs (line in red) and free DHLA (line in blue). The absorbance spectrum of the DHLA-capped HgSe NPs is also included (line in black).

The determination of the molar extinction coefficient of nanocrystals enables to perform fast and simple concentration determinations of NPs by just UV-vis absorption measurements. Thus, the molar extinction coefficient of the synthesized NPs was determined from the absorbance values at the excitonic absorption shoulder (390 nm) plotted as a function of the different molar concentrations of the NPs assayed (Fig. S9 in the ESI†). Samples containing NPs at different concentrations were prepared from a stock solution of DHLA-capped HgSe NPs (9.5 nM), characterized by ICP-MS, HR-TEM and XRD. The slope of the regression line (extinction coefficient of the DHLA-capped HgSe NPs sample) turned out to be 2521 ± 6 (×10^5) M^{-1} cm^{-1} (1SD, $n = 3$). In this way, for future bioanalytical applications of such water-solubilized HgSe NPs, as the molar extinction coefficient is known, a simply measurement of the absorbance at 390 nm would directly give the number nanoparticle concentration of the working solution.

DHLA–HgSe NPs analysis by AF4 on-line coupled to fluorescence and ICP-MS

AF4 is a separation technique that provides a size-dependent separation and characterization of nanoscale particles dispersed in aqueous media.[38] It has demonstrated its great potential to separate different types of NPs with a low risk of sample degradation or aggregation due to the minimal interaction with the separation membrane.[29,38] Furthermore, coupling the AF4 to fluorescence and sensitive elemental specific detectors, such as ICP-MS, could provide not only a nanoparticle size separation but also molecular and elemental information[29] of the DHLA–HgSe NPs in the aqueous phase.

The obtained fractogram of the DHLA-capped HgSe NPs is shown in Fig. 6. It is apparent that there is only one peak eluting at ~34 min, which could correspond with a unique population of DHLA–HgSe NPs. As expected, this peak contained the two elements monitored, Hg and Se. Interestingly, the elemental molar ratio of the nanoparticle population could be determined using external FIA calibration and inorganic standards. In this

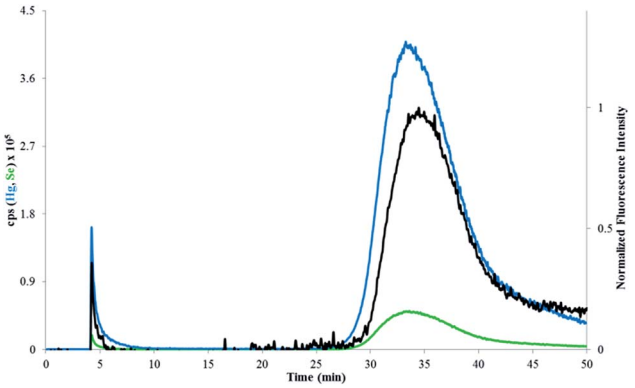

Fig. 6 Fractogram of the DHLA-capped HgSe NPs with fluorescence detection at 575 nm (line in black) and ICP-MS detection: ^{202}Hg (line in blue) and ^{80}Se (line in green).

sense, the obtained Se/Hg molar ratio was 0.98 ± 0.01 (1SD, $n = 3$), which matches well with the values obtained previously by the other techniques used in this study. Unfortunately, S information could not be obtained as we resorted to a small amount of an anionic surfactant such as SDS in the carrier (0.01%, w/v) in order to prevent nanoparticle aggregation and minimize the interactions between HgSe NPs and the permeation membrane. Additionally, a significant fluorescence emission at 575 nm was observed in such population of NPs. Undesired populations were not observed neither in the fluorescence nor ICP-MS fractograms. Therefore, the coupling between AF4 with fluorescence and ICP-MS allowed to corroborate not only that the derivatized DHLA–HgSe NPs were stable and still fluorescent in a salt-containing and dynamic water medium but also the slight molar excess of Hg in the NP and the presence of a single nanoparticle population.

Conclusions

HgSe NPs, synthesized *via* a sonochemical method, have been here transferred successfully to a water medium using DHLA as the capping ligand. Both morphology and crystal structure of the engineered NPs have been characterized by HR-TEM, XRD and XPS techniques. DLS, FT-IR, ^{1}H-NMR and EDX complementary analysis confirmed that the thiol-containing ligands were incorporated on the surface of the HgSe NPs. The resulting DHLA-capped NPs showed high stability and a strong fluorescent emission in solution as assessed and confirmed by the zeta potential and AF4 results observed.

ICP-MS was used to determine accurately the elemental molar ratio of the engineered DHLA–HgSe NPs. Moreover, nanoparticle number concentration and the ligand density of the DHLA-capped HgSe NPs, in terms of number of ligands per nanoparticle, have been precisely determined here using for the first time the triple quadrupole ICP-MS capabilities to detect simultaneously Hg, Se and especially S, with high sensitivity and minimal interferences.

The comprehensive characterization of the native and DHLA-derivatized HgSe NPs synthesized in this work together with their proven stability in water media (demonstrated by DLS, zeta potential and AF4 studies) opens the door to the possibility of reproducible environmental and/or toxicological studies of HgSe NPs, shedding light into their formation in animal tissues. Interestingly, the newly produced aqueous-stable DHLA–HgSe NPs are fluorescent, which make them ideal to investigate their fate and interactions in biological systems.

Acknowledgements

This work was supported by the Spanish Ministry of Education (MINECO-13-CTQ2013-49032-C2-1-R) and Principado de Asturias (FC-15-GRUPIN14-092). Agilent Technologies Foundation is also acknowledged. Diego Bouzas-Ramos and Mario Menéndez-Miranda acknowledge the Ph.D. grants (BP14-137 and BP12-046, respectively) from Principado de Asturias (Spain).

References

1 J. Parízek and I. Ostádalová, *Experientia*, 1967, **23**, 142–143.
2 D. Y. Yang, Y. W. Chen, J. M. Gunn and N. Belzile, *Environ. Rev.*, 2008, **16**, 71–92.
3 M. A. K. Khan and F. Wang, *Environ. Toxicol. Chem.*, 2009, **28**, 1567–1577.
4 J. H. Koeman, W. H. M. Peeters, C. H. M. Koudstaal-Hol, P. S. Tjioe and J. J. M. de Goeij, *Nature*, 1973, **245**, 385–386.
5 L. Kosta, A. R. Byrne and V. Zelenko, *Nature*, 1975, **254**, 238–239.
6 R. Martoja and J. P. Berry, *Vie et Milieu*, 1980, **30**, 7–10.
7 M. A. K. Khan and F. Wang, *Chem. Res. Toxicol.*, 2010, **23**, 1202–1206.
8 A. M. Asaduzzaman and G. Schreckenbach, *Inorg. Chem.*, 2011, **50**, 2366–2372.
9 M. A. K. Khan and F. Wang, *Chem. Res. Toxicol.*, 2009, **22**, 1827–1832.
10 A. J. Rawson, J. P. Bradley, A. Teetsov, S. B. Rice, E. M. Haller and G. W. Patton, *Ecotoxicol. Environ. Saf.*, 1995, **30**, 309–314.
11 E. Nakazawa, T. Ikemoto, A. Hokura, Y. Terada, T. Kunito, S. Tanabe and I. Nakai, *Metallomics*, 2011, **3**, 719–725.
12 M. Nigro and C. Leonzio, *Mar. Ecol.: Prog. Ser.*, 1996, **135**, 137–143.
13 M. Korbas, J. L. O'Donoghue, G. E. Watson, I. J. Pickering, S. P. Singh, G. J. Myers, T. W. Clarkson and G. N. George, *ACS Chem. Neurosci.*, 2010, **1**, 810–818.
14 P. Rivera-Gil, G. Oberdörster, A. Elder, V. Puntes and W. J. Parak, *ACS Nano*, 2010, **4**, 5527–5531.
15 S. J. Soenen, P. Rivera-Gil, J. M. Montenegro, W. J. Parak, S. C. De Semedt and K. Braeckmans, *Nano Today*, 2011, **6**, 446–465.
16 C. M. Sayes and D. B. Warheit, *Wiley Interdiscip. Rev.: Nanomed. Nanobiotechnol.*, 2009, **1**, 660–670.
17 T. Ohmiya and Y. Suge, *Jpn. J. Appl. Phys.*, 1970, **9**, 840–841.
18 I. K. Taimni and G. B. S. Salaria, *Anal. Chim. Acta*, 1955, **12**, 519–525.
19 J. Li, Z. Chen, R. J. Wang and D. M. Proserpio, *Coord. Chem. Rev.*, 1999, **190–192**, 707–735.

20 Y. Li, Y. Ding, H. Liao and Y. Qian, *J. Phys. Chem. Solids*, 1999, **60**, 965–968.
21 M. Esmaeili-Zare, M. Salavati-Niasari, D. Ghanbari and A. Aminifazl, *J. Cluster Sci.*, 2013, **24**, 881–890.
22 T. Ding, J. J. Zhu and J. M. Hong, *Mater. Lett.*, 2003, **57**, 4445–4449.
23 H. Wang, S. Xu, X. N. Zhao, J. J. Zhu and X. Xin, *Mater. Sci. Eng., B*, 2002, **96**, 60–64.
24 K. S. Suslick, *Science*, 1990, **247**, 1439–1445.
25 M. Kristl and M. Drofenik, *Ultrason. Sonochem.*, 2008, **15**, 695–699.
26 M. Esmaeili-Zare, M. Salavati-Niasari and A. Sobhani, *J. Ind. Eng. Chem.*, 2014, **20**, 3518–3523.
27 H. Hinterwirth, S. Kappel, T. Waitz, T. Prohaska, W. Lindner and M. Lämmerhofer, *ACS Nano*, 2013, **7**, 1129–1136.
28 A. R. Clapp, E. R. Goldman and H. Mattoussi, *Nat. Protoc.*, 2006, **1**, 1258–1266.
29 M. Menéndez-Miranda, M. T. Fernández-Argüelles, J. M. Costa-Fernández, J. R. Encinar and A. Sanz-Medel, *Anal. Chim. Acta*, 2014, **839**, 8–13.
30 S. D. Fernández, N. Sugishama, J. R. Encinar and A. Sanz-Medel, *Anal. Chem.*, 2012, **84**, 5851–5857.
31 R. Rai, W. Maher and F. Kirkowa, *J. Anal. At. Spectrom.*, 2002, **12**, 1560–1563.
32 K. Okitsu, Y. Mizukoshi, H. Bandow, Y. Maeda, T. Yamamoto and Y. Nagata, *Ultrason. Sonochem.*, 1996, **3**, S249–S251.
33 W. H. Zhang, J. Yang and J. S. Yu, *J. Mater. Chem.*, 2012, **22**, 6383–6388.
34 S. Honary and F. Zahir, *Trop. J. Pharm. Res.*, 2013, **12**, 265–273.
35 Y. Yu, K. Zhang, Z. Li and S. Sun, *Opt. Mater.*, 2012, **34**, 793–798.
36 T. Pons, H. T. Uyeda, I. L. Medintz and H. Mattoussi, *J. Phys. Chem. B*, 2006, **110**, 20308–20316.
37 A. R. Montoro, J. R. Encinar, M. T. Fernández-Argüelles, J. M. Costa-Fernández and A. Sanz-Medel, *Chem. Commun.*, 2009, 3107–3109.
38 J. Gigault, J. M. Pettibone, C. Schmitt and V. A. Hackley, *Anal. Chim. Acta*, 2014, **809**, 9–24.